

Eavesdropping time and frequency: phase noise cancellation along a time-varying path, such as an optical fiber

Gesine Grosche

Physikalisch-Technische Bundesanstalt, Bundesallee 100, D-38116 Braunschweig, Germany (gesine.grosche@ptb.de)

Received March 4, 2014; accepted March 8, 2014;

posted March 14, 2014 (Doc. ID 207644); published April 17, 2014

Single-mode optical fiber is a highly efficient connecting medium used not only for optical telecommunications but also for the dissemination of ultrastable frequencies or timing signals. Ma *et al.* [Opt. Lett. **19**, 1777 (1994)] described a measurement and control system to deliver the same optical frequency at *two* places, namely the two ends of a fiber, by eliminating the “fiber-induced phase-noise modulation, which corrupts high-precision frequency-based applications.” I present a simple detection and control scheme to deliver the same optical frequency at *many* places anywhere along a transmission path, or in its vicinity, with a relative instability of 1 part in 10^{19} . The same idea applies to radio frequency and timing signals. This considerably simplifies future efforts to make precise timing or frequency signals available to many users, as required in some large-scale science experiments. © 2014 Optical Society of America

OCIS codes: (060.2360) Fiber optics links and subsystems; (060.2840) Heterodyne; (120.3940) Metrology.
<http://dx.doi.org/10.1364/OL.39.002545>

Optical frequency references and clocks have achieved an unprecedented accuracy of better than 1 part in 10^{17} [1,2], with an instability near 1 part in 10^{18} [3]. They are formidable tools for precision experiments, which often rely on converting the quantity to be measured into a frequency. Some of the most fundamental questions in physics relate to quantities of energy, space, and time, and these quantities are directly related to frequency (and/or phase). This makes experiments probing fundamental questions accessible to frequency or phase measurements, for example testing for time variations of fundamental constants [4] or large-area Sagnac interferometers [5]. A prominent example is relativistic geodesy, that is, the measurement of gravitational redshift with optical clocks [6]. We therefore wish to transfer timing or frequency signals to other experimental sites, enabling applications outside metrology [4–7].

To date, efforts have focused on long-distance connections [8–10] between just two points, one “remote” lab and one “local” lab connected by an optical fiber, using methods similar to that proposed in 1994 by Ma *et al.* [11] to correct phase perturbations between the local and remote end. For example, we have transmitted optical frequencies with a relative accuracy of 10^{-19} over 146 km deployed fiber [12] and remotely characterized optical clock lasers online with hertz-level resolution [13]. Significant efforts are now underway to establish national and even international metrology fiber networks.

One important question [14–19] is how to distribute reference frequencies to many users simultaneously in a cost-effective way. Surprisingly, with one point-to-point connection (such as a long stabilized fiber), we can “tap” this fiber anywhere and locally derive a reference frequency with the same precision as that achieved at the end point [18]. We present the patented concept, an experimental setup achieving relative frequency instability of 10^{-19} , and several extensions of the idea; these include a branching design and the multipoint dissemination of time using two-way transfer. The methods complement the Ethernet-based “White Rabbit” [19] and

enable high-fidelity distribution of frequency or time even for large-area science projects, such as radio telescope arrays [7] or national metrology networks.

To explain the basic idea, we first consider the existing scheme for point-to-point stabilization. Figure 1 shows a commonly implemented and well-characterized method for phase-stable transmission of an ultrastable optical frequency ν_{local} from a local point A to a remote point Z [8–10,12,20]. Analogous, earlier designs enable the phase-stable transmission of radio frequency [21,22] or pulsed [23] signals. The method is reminiscent of [11,24] (though different) and can be understood by viewing the entire transmission path from A to the mirror at Z as the long arm of an interferometer.

We denote by $\Delta\phi_{ij}$ the phase shift experienced by a signal travelling from any point i to point j and assume symmetry of the transmission path: $\Delta\phi_{ij} = \Delta\phi_{ji}$. The acousto-optic modulator (AOM) AOM2 provides a fixed frequency shift to distinguish light that has reached the mirror at Z from light reflected anywhere else along the transmission path. At photodetector DetA, the returned light is superimposed with local light traveling through a short reference arm. This yields a beat signal with frequency

$$f_{\text{DetA}} = 2(f_{\text{AOM1}} + \Delta\dot{\phi}_{AZ}/2\pi + f_{\text{AOM2}})$$

and phase reflecting the momentary phase difference between the two interferometer arms. The beat signal f_{DetA} is compared to a synthesized signal at frequency f_{synth} with a phase-frequency comparator [21] or a simple mixer. A servo acts on the phase and frequency of AOM1 to maintain a constant phase difference between the beat signal and the synthesizer signal, resulting in a fixed phase relationship (modulo the frequency offset $f_{\text{synth}}/2$) between light at point Z and at point A. Thus the frequency delivered to point Z is given by $\nu_Z = \nu_{\text{local}} + f_{\text{synth}}/2 = \nu_A + f_{\text{synth}}/2$.

To generate a phase-stable signal at an intermediate point C along the transmission path, we now tap the

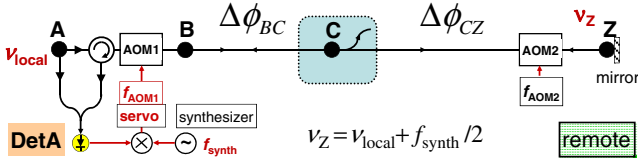


Fig. 1. Stabilized fiber link connecting the remote point Z with the local point A. For a detailed discussion, see for instance [8,20].

transmitted signal in both directions. Figures 1 and 2 and the analysis describe in detail one implementation ([18], p. 2); similar setups are suitable for periodically modulated or pulsed signals [18]. Here the terminology of optical frequency transfer is used.

The forward propagating light has frequency

$$\nu_f := \nu_{C-f} = \nu_A + f_{\text{AOM1}} + \Delta\phi_{\text{AC}}/2\pi,$$

whereas backward propagating light has frequency

$$\nu_b := \nu_{C-b} = \nu_A + f_{\text{AOM1}} + \Delta\dot{\phi}_{\text{AZ}}/2\pi + 2f_{\text{AOM2}} + \Delta\dot{\phi}_{\text{ZC}}/2\pi.$$

We superimpose forward- and backward propagating light on photodetector DetC (here ignoring noise beyond the tapping point) to generate a beat signal at frequency

$$\begin{aligned} \nu_b - \nu_f &= \Delta\dot{\phi}_{\text{CZ}}/2\pi + 2f_{\text{AOM2}} + \Delta\dot{\phi}_{\text{ZC}}/2\pi \\ &= 2(\Delta\dot{\phi}_{\text{CZ}}/2\pi + f_{\text{AOM2}}). \end{aligned} \quad (1)$$

The beat signal is amplified and its frequency digitally divided by two. Applying this as a correction frequency $f_{\text{corr}} := (\nu_b - \nu_f)/2$ to the forward propagating light at point C, for instance using another AOM, we obtain a stable signal at point C:

$$\nu_{\text{C-out}} = \nu_f + f_{\text{corr}} = \nu_Z = \nu_{\text{local}} + f_{\text{synth}}/2.$$

This can be viewed as detecting at point C the additional phase shift between points C and Z, and applying this to the signal coupled out at point C, so that its frequency and phase follow those of the signal at point Z. The output at point C is thus ideally as stable as ν_Z . Since $\nu_Z = (\nu_b + \nu_f)/2$, applying $-f_{\text{corr}}$ to the backward propagating light at point C also yields ν_Z [15,18].

The design has several useful properties. Many access points D, E, ... may be operated along a single stabilized

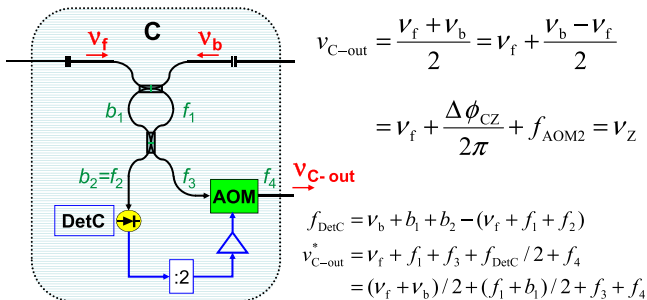


Fig. 2. Signal generation at point C, from signals tapped in forward and backward directions, with frequencies ν_f and ν_b .

link at small extra cost for each. While [16] introduces extra frequencies, here the main link is unchanged. The signal processing is a simple and robust feed-forward system, which automatically works continuously and allows a free choice of correction bandwidth; in contrast to [16,17] it requires no additional stabilization.

Furthermore, high-power ultrastable light can be made available [18]. If we wish to preserve optical power in the main link, asymmetric beam splitters or tap couplers extract only a small percentage of the light. The extracted power may be boosted, for example with an erbium-doped fiber amplifier before detector DetC. Alternatively, the weak ($\sim\mu\text{W}$) extracted signals are first superimposed with light from a laser at frequency ν_{L0} giving two strong heterodyne beat signals $\nu_b - \nu_{L0}$ and $\nu_f - \nu_{L0}$. Their difference frequency is again $\nu_b - \nu_f$ and is independent of ν_{L0} and its fluctuations. As before, after division by two, it may serve as a correction frequency. Alternatively, if the mean frequency of the two heterodyne beat signals, $(\nu_b - \nu_{L0} + \nu_f - \nu_{L0})/2$, is added as a correction to ν_{L0} (e.g., via an AOM), we obtain ultrastable, high-power laser light at frequency $\nu_L = \nu_Z$.

Key advantages of the scheme are its simple installation and its monitoring capability. By locating point Z in a second metrology lab, or even next to the input, thus forming a loop A-Z, the main link stabilization may be tested and optimized to reach the physical limits [20] and to verify its accuracy. Later, the same setup monitors the link performance and allows online verification and assessment of the frequency distribution.

The new scheme was tested using a narrow-linewidth (<5 kHz) optical source (Koheras Adjustik fiber laser) at a frequency near 194.3 THz, on a short but intrinsically noisy fiber link. This allows exploring the fiber noise suppression and detecting system noise contributions. Our test link is a combination of a 10 m spool wound around a thin metal drum and 100 m exposed fiber going to another laboratory (some 40 m away) and back. Point C is located at the input of the 100 m fiber. Touching or wriggling this fiber, or the fiber section wound around the drum, introduces massive phase noise, visible as a beat linewidth of several kilohertz. In initial, separate experiments, which served to verify the new scheme, we also used an AOM to introduce large and well-defined perturbations.

The overall configuration is as shown in Figs. 1 and 2, but with the remote point Z and local point A located in the same laboratory. We stabilize A \rightarrow Z with the standard scheme and measure the remote frequency ν_Z . We also record the output frequency $\nu_{\text{C-out}}$ at the intermediate point C using the new scheme, and, additionally, the frequency correction f_{corr} applied to the AOM at point C. f_{corr} shows the fluctuations of the free-running link between points C and Z. All beat frequencies are recorded with totalizing counters (Kramer + Klische FXE; Π -type operation [25]), to give a time sequence of frequency values from which we calculate the frequency instability (Allan deviation, ADEV, [25]).

Open diamonds in Fig. 3 show the frequency instability at point C when implementing the new scheme as shown in Figs. 1 and 2; $\nu_{\text{C-out}}$ reaches a relative instability (ADEV in >10 kHz bandwidth) of 10^{-17} after 1000 s.

Free-running fiber noise (full green triangles, f_{corr}) is clearly suppressed.

However, $\text{ADEV}(\nu_{C\text{-out}})$ shows a plateau from 10... 100 s, characteristic of uncompensated fiber paths [26], and the instability of $\nu_{C\text{-out}}$ is roughly 10 times that of ν_Z (small black circles). A similar, but higher, plateau of excess instability was reported in [14], using a modified implementation of this scheme [18] but operating at radio frequencies; a plateau was also seen recently in [15], reaching 4×10^{-18} at 10000 s with a modified optical implementation. Our excess instability falls below 10^{-18} at 10000 s. Since end-point optical fiber links are feasible at the 10^{-19} level [9,10,12] even for long distances, and the newest optical clocks [1–3] achieve an instability near 10^{-18} , we wish to eliminate this excess noise.

Analysis of the fiber paths that contribute to frequency fluctuations at point C, see Fig. 2, shows that $\nu_{C\text{-out}} = (\nu_f + \nu_b)/2 + (f_1 + b_1)/2 + f_3 + f_4$. [Notation: we write f_1 etc., for both the fiber paths and the frequency fluctuations arising from them.] The total length of exposed, uncompensated fiber is $\sim 2\text{--}3$ m. An improved design, which minimizes uncompensated fiber paths, is shown in Fig. 4.

For this design (full blue squares in Fig. 3), $\nu_{C\text{-out}}$ is as stable as ν_Z for short times (10^{-17} at 10 s); the excess frequency instability at 1000 s is below 10^{-18} . After 10000 s, an instability below 10^{-19} is reached; this is a factor 40 lower than reported in [15]. The total uncompensated fiber length (Fig. 4) was below 0.8 m, with f_2, f_3 , and part of f_4 being colocated inside a box to minimize air currents and mounted on a 12 mm thick aluminum board as a thermal mass. Further noise reduction is possible by environmental shielding, length-matching fibers so temperature changes enter common mode ($f_2 \sim f_3 + f_4$), and/or active temperature stabilization.

Reaching the 10^{-19} instability level, this proof-of-principle experiment demonstrates that the scheme supports state-of-the-art clock comparisons. A simplified analysis of the delay limit [20] gives the same precision (or, actually *better* precision, see recent analysis and experimental results in [27]) at the intermediate point as at the end point. Further aspects relating to polarization

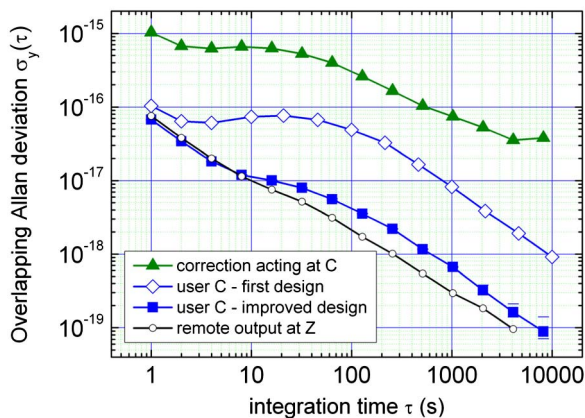


Fig. 3. Measured frequency instability (ADEV). Green triangles: f_{corr} , represents free-running fiber (see text); black open circles: ν_Z , stabilized remote output at Z; blue open diamonds: $\nu_{C\text{-out}}$, stabilized output at point C, first design; full blue squares: $\nu_{C\text{-out}}$ for the improved design.

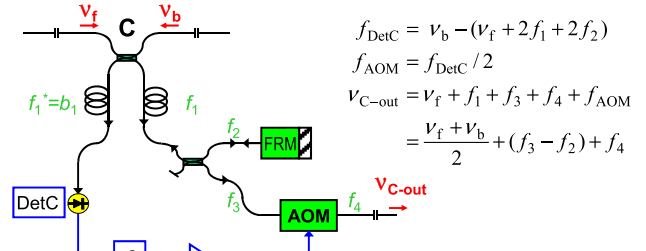


Fig. 4. Improved “tentacle” design for detection unit. FRM, Faraday rotator mirror; AOM, acousto-optic modulator; DetC, photodetector. Fiber paths f_1 and b_1 contribute no noise to $\nu_{C\text{-out}}$.

and effects of link asymmetry will be discussed elsewhere. We call the improved version the “tentacle” design: extra paths (or “tentacles”) f_1 and b_1 at point C that deliver $\nu_{C\text{-out}}$ no longer introduce *any* additional noise but cancel completely. Thus, f_1 and b_1 may be made long, enabling a true branching distribution from a fiber backbone link, which reaches into the vicinity of the main transmission path.

Like the original point-to-point method, the basic idea of the current scheme is not restricted to optical fibers but is applicable to any time-varying signal path of sufficient symmetry—in particular, it is well suited for free-space connections [18]. Similarly, dissemination of an optical carrier frequency is just a special case. The same principles apply for any periodic signal (such that we can define a phase $\Delta\phi_{ij}$), including pulsed signals [23], radio frequency modulation (as recently implemented in [14]), and any signals modulated onto such carriers, or even the simultaneous dissemination of several frequencies [18]. In consequence, *synchronization* of many locations may be realized, for instance by using a slowly chirped optical frequency on a stabilized fiber link [28] combined with the scheme above.

A much more general application follows without *stabilized* transmission paths, instead tapping a two-way time and frequency transfer (TWTFT) link [29]; we call this “eavesdropping” time (and frequency), see Fig. 5.

Classic TWTFT, first demonstrated via the Telstar 1 satellite 50 years ago [30] and later implemented via fiber [29], uses counterpropagating signals sent and received by the two end points A and Z. The time difference between sending and receiving is measured by time interval counters (TICs) at point A and point Z to give the clock difference (simplified from [29,31]):

$$\text{clockA} - \text{clockZ} = (\text{TICA} - \text{TICZ})/2 - (\tau_{ZA} - \tau_{AZ})/2,$$

where τ_{AZ} is the signal delay between A and Z. For a symmetric link ($\tau_{ZA} = \tau_{AZ}$), this directly allows clock

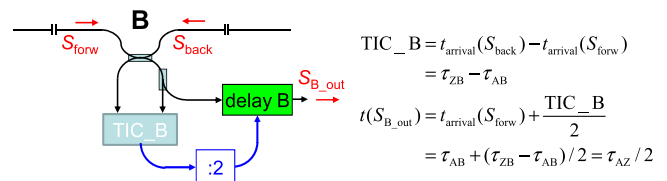


Fig. 5. Eavesdropping on a TWTFT link between points A and Z, which simultaneously send signals S_{forw} and S_{back} . At each extraction point, signal S_{Bout} exits the apparatus at time $\tau_{AZ}/2$.

synchronization, that is $\text{clockZ}' = \text{clockA}$, so both end points can send a signal at the same time and know τ_{AZ} . Now we tap these forward and backward travelling signals, at any point B (here chosen closer to A than Z), and measure the time difference for signal arrival $\text{TICB} := t_{\text{arrival}}(S_{\text{Bback}}) - t_{\text{arrival}}(S_{\text{Bforw}}) = \tau_{ZB} - \tau_{AB}$. If we delay the forward extracted signal at B by $(1/2)\text{TICB}$, it will exit our apparatus at point B at $t(S_{\text{Bout}}) = (\tau_{AB} + (\tau_{ZB} - \tau_{AB})/2) = \tau_{AZ}/2$, in the timescale given by clockA (and clockZ'). Note that all points along a link can be synchronized to each other without τ_{AZ} being known, or even stable, simply by eavesdropping: all points experience the same offset $\tau_{AZ}/2$. They share reference frequencies provided by A or Z. If they are additionally given the information of τ_{AZ} , they may synchronize to the reference time scale of clockA.

Implementation may use receiver modules of standard TWTFM-modems, as in point-to-point fiber-based time transfer [32,33] or newly developed electronic delay lines and time signal encoders/decoders [34].

In summary, we have presented new methods which—using very little extra instrumentation—make available at intermediate points along or near a transmission path the same timing or frequency signals that previously could only be delivered to its end points. Specifically, for applications requiring the highest precision, we demonstrated delivering an optical frequency to an intermediate point with relative instability 1×10^{-17} (10 s) and 10^{-19} (10000 s). An improved branching design reaches users in the vicinity of a point-to-point fiber link. If a ring topology is used, the scheme enables monitored time and frequency dissemination to many users. The idea is applicable to any time-varying signal path, and we have outlined how to apply it, for example, to classic two-way time and frequency transfer links with intermediate access.

I am indebted to Fritz Riehle and Giorgio Santarelli for their indefatigable enthusiasm and openness to new ideas, to the authors of [11] for lucid writing, and to the Deutsche Forschungsgemeinschaft (SFB 407 and QUEST, Centre for Quantum Engineering and Space-Time Research) and the European Space Agency for financial support.

References

1. C. W. Chou, D. B. Hume, J. C. J. Koelemeij, D. J. Wineland, and T. Rosenband, *Phys. Rev. Lett.* **104**, 070802 (2010).
2. B. J. Bloom, T. L. Nicholson, J. R. Williams, S. L. Campbell, M. Bishof, X. Zhang, W. Zhang, S. L. Bromley, and J. Ye, *Nature* **506**, 71 (2014).
3. N. Hinkley, J. A. Sherman, N. B. Phillips, M. Schioppa, N. D. Lemke, K. Beloy, M. Pizzocaro, C. W. Oates, and A. D. Ludlow, *Science* **341**, 1215 (2013).
4. S. G. Karshenboim, *Can. J. Phys.* **83**, 767 (2005).
5. C. Clivati, D. Calonico, G. A. Costanzo, A. Mura, M. Pizzocaro, and F. Levi, *Opt. Lett.* **38**, 1092 (2013).
6. T. C. W. Chou, D. B. Hume, T. Rosenband, and D. J. Wineland, *Science* **329**, 1630 (2010).
7. P. E. Dewdney, P. J. Hall, R. T. Schilizzi, and T. J. L. W. Lazio, *Proc. IEEE* **97**, 1482 (2009).
8. N. R. Newbury, P. A. Williams, and W. Swann, *Opt. Lett.* **32**, 3056 (2007).
9. O. Lopez, A. Haboucha, B. Chanteau, C. Chardonnet, A. Amy-Klein, and G. Santarelli, *Opt. Express* **20**, 23518 (2012).
10. K. Predehl, G. Grosche, S. M. F. Raupach, S. Droste, O. Terra, J. Alnis, T. Legero, T. W. Hänsch, T. Udem, R. Holzwarth, and H. Schnatz, *Science* **336**, 441 (2012).
11. L. S. Ma, P. Jungner, J. Ye, and J. L. Hall, *Opt. Lett.* **19**, 1777 (1994).
12. G. Grosche, O. Terra, K. Predehl, R. Holzwarth, B. Lipphardt, F. Vogt, U. Sterr, and H. Schnatz, *Opt. Lett.* **34**, 2270 (2009).
13. A. Pape, O. Terra, J. Friebe, M. Riedmann, T. Wübbena, E. M. Rasel, K. Predehl, T. Legero, B. Lipphardt, H. Schnatz, and G. Grosche, *Opt. Express* **18**, 21477 (2010).
14. C. Gao, B. Wang, W. L. Chen, Y. Bai, J. Miao, X. Zhu, T. C. Li, and L. J. Wang, *Opt. Lett.* **37**, 4690 (2012).
15. Y. Bai, B. Wang, X. Zhu, C. Gao, J. Miao, and L. J. Wang, *Opt. Lett.* **38**, 3333 (2013).
16. S. W. Schemm, D. Gozzard, K. G. H. Baldwin, B. J. Orr, R. B. Warrington, G. Aben, and A. N. Luiten, *Opt. Lett.* **38**, 2893 (2013).
17. P. Krehlik, L. Sliwczynski, L. Buczek, and M. Lipinski, *IEEE Trans. Ultrason. Ferroelectr. Freq. Control* **60**, 1804 (2013).
18. G. Grosche, "Verfahren zum Bereitstellen einer Referenzfrequenz," German patent DE 200810062139 (June 24, 2010).
19. <http://www.ohwr.org/projects/white-rabbit>.
20. P. A. Williams, W. C. Swann, and N. R. Newbury, *J. Opt. Soc. Am. B* **25**, 1284 (2008).
21. M. Musha, Y. Sato, K. Nakagawa, K. Ueda, A. Ueda, and M. Ishiguro, *Appl. Phys. B* **82**, 555 (2006).
22. F. Narbonne, M. Lours, S. Bize, A. Clairon, G. Santarelli, O. Lopez, C. Daussy, A. Amy-Klein, and C. Chardonnet, *Rev. Sci. Instrum.* **77**, 064701 (2006).
23. G. Marra, H. S. Margolis, and D. J. Richardson, *Opt. Express* **20**, 1775 (2012).
24. J. Ye, J. L. Peng, R. J. Jones, K. W. Holman, J. L. Hall, D. J. Jones, S. A. Diddams, J. Kitching, S. Bize, J. C. Bergquist, L. W. Hollberg, L. Robertsson, and L. S. Ma, *J. Opt. Soc. Am. B* **20**, 1459 (2003).
25. S. T. Dawkins, J. J. McFerran, and A. N. Luiten, *IEEE Trans. Ultrason. Ferroelectr. Freq. Control* **54**, 918 (2007).
26. G. Grosche, B. Lipphardt, and H. Schnatz, *Eur. Phys. J. D* **48**, 27 (2008).
27. A. Bercy, S. Guellati-Khelifa, F. Stefani, G. Santarelli, C. Chardonnet, P.-E. Pottie, O. Lopez, and A. Amy-Klein, *J. Opt. Soc. Am. B* **31**, 678 (2014).
28. S. M. F. Raupach and G. Grosche, "Chirped frequency transfer with an accuracy of 10^{-18} and its application to the remote synchronisation of timescales," arXiv: 1308.6725 (2013).
29. S. A. Jefferts, M. A. Weiss, J. Levine, S. Dilla, E. W. Bell, and T. E. Parker, *IEEE Trans. Instrum. Meas.* **46**, 209 (1997).
30. J. M. A. Steele, W. Markowitz, and C. A. Lidback, *IEEE Trans. Instrum. Meas.* **13**, 164 (1964).
31. D. Kirchner, H. Ressler, P. Grudler, F. Baumont, C. Veillet, W. Lewandowski, W. Hanson, W. Klepczynski, and P. Urich, *Metrologia* **30**, 183 (1993).
32. M. Rost, D. Piester, W. Yang, T. Feldmann, T. Wübbena, and A. Bauch, *Metrologia* **49**, 772 (2012).
33. O. Lopez, A. Kanj, P. E. Pottie, D. Rovera, J. Achkar, C. Chardonnet, A. Amy-Klein, and G. Santarelli, *Appl. Phys. B* **110**, 3 (2013).
34. L. Sliwczynski, P. Krehlik, A. Czubla, L. Buczek, and M. Lipinski, *Metrologia* **50**, 133 (2013).